forests

MDPI

Article

Morphological Characteristics and Transcriptome Comparisons of the Shoot Buds from Flowering and Non-Flowering *Pleioblastus pygmaeus*

Wenjing Yao [1], Chuanzhe Li [2], Shuyan Lin [1,*], Li Ren [1], Yawen Wan [1], Li Zhang [1] and Yulong Ding [1]

[1] Co-Innovation Center for Sustainable Forestry in Southern China/Bamboo Research Institute, Nanjing Forestry University, 159 Longpan Road, Nanjing 210037, China; yaowenjing@njfu.edu.cn (W.Y.); renli199433@163.com (L.R.); yawwan@126.com (Y.W.); yaowenjing1988@126.com (L.Z.); ylding@vip.163.com (Y.D.)

[2] Institute of Agricultural Resources and Environment, Jiangsu Academy of Agricultural Sciences, 50 Zhongling Street, Nanjing 210014, China; lichuanzhe66@163.com

* Correspondence: lrx@njfu.com.cn

Received: 19 October 2020; Accepted: 19 November 2020; Published: 23 November 2020

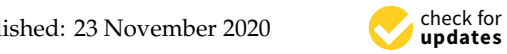

Abstract: Bamboo plants have a distinctive life cycle with long flowering periodicity. Many species remain in vegetative growth for decades, followed by large-scale flowering and subsequent death. Floral transition is activated while shoot buds are still dormant in bamboo plants. In this study, we performed morphological characterization and transcriptome analysis of the shoot buds at different growth stages from flowering and non-flowering *Pleioblastus pygmaeus*. The morphological and anatomical structures of the dormant shoot buds were similar in flowering and non-flowering plants, while there was an obvious difference between the flower buds from flowering plants and the leaf buds from non-flowering plants. The transcriptomes of the dormant shoot buds, germinated shoots, and flower buds from flowering *P. pygmaeus*, and the dormant shoot buds, germinated shoots, and leaf buds from non-flowering *P. pygmaeus* were profiled and compared by RNA-Seq. The identified sequences were mostly related to metabolic synthesis, signal transmission, translation, and other functions. A total of 2434 unigenes involved in different flowering pathways were screened from transcriptome comparisons. The differentially expressed unigenes associated with the photoperiod pathway were related to circadian rhythm and plant hormone signal transduction. Moreover, the relative expression levels of a few key flowering-related genes such as *CO*, *FT*, *FLC*, and *SOC1* were quantified by *q*RT-PCR, which was in accordance with RNA-Seq. The study revealed morphological differences in the shoot buds at different growth stages and screened flowering-related genes by transcriptome comparisons of the shoot buds from flowering and non-flowering *P. pygmaeus*, which will enrich the research on reproductive biology of bamboo plants and shed light on the molecular mechanism of the floral transition in bamboo plants.

Keywords: *Pleioblastus pygmaeus*; flowering pathways; shoot buds; floral transition; RNA-Seq

1. Introduction

As an important forest resource with the advantages of rapid growth, strong adaptability and great reproduction ability, bamboo plants play an irreplaceable role in alleviating wood resource shortages, protecting the ecological environment and promoting ecological civilization construction [1,2]. Bamboo plants are perennial flowering plants with long flowering cycles varying from a few years to several decades [2]. The flowering process may lead to large-scale death of bamboo plants or even the

whole forest, which can cause huge economic losses and induce soil erosion [2,3]. Due to the unique reproductive characteristics, study on flowering has always been a research hotspot in bamboo plants.

Previous studies on reproductive biology of bamboo plants mainly focused on somatic embryogenesis, pollen viability, flowering bud differentiation, etc. [4–6]. Developmental biology has explored the changes of floral organ structure and physiological indicators during the flowering period [7,8]. With the population of high-throughput sequencing and the release of the genome resource of *Phyllostachys edulis* (Carrière) J.Houz., 1906 in 2013, more and more studies have shifted to the molecular mechanism of bamboo flowering by transcriptome analysis in recent years [9,10]. For example, the transcriptome of *Fargesia macclureana* (Bor) Stapleton, 1983 inflorescences was firstly profiled to investigate the putative mechanisms underlying flowering time [11]. The transcriptome data of flowering tissues of *P. edulis* was analyzed to screen key genes involved in the flowering process [12]. Zhang et al. (2018) firstly investigated the transcriptome of *Dendrocalamus latiflorus* Munro, 1868 inflorescences to identify gene expression patterns during flower development [13]. RNA-Seq analysis of panicle and vegetative tissues from moso bamboo showed 30% of flowering-related genes were transcription factor (TF) genes, heat shock protein genes, and stress-related genes [14]. Increasing reports on identification of flowering-related genes through the transcriptome profile of flowering tissues appeared in different bamboo species. Meanwhile, floral transition is activated while the shoot buds are still dormant in bamboo plants. However, the research on identifying flowering-related genes through transcriptome screening of the shoot buds is limited in bamboo plants.

Pleioblastus pygmaeus (Miq.) Nakai, 1932 is a kind of small-size ornamental bamboo species that is widely used in landscape architecture and has high ecological and economic value [5]. In this study, morphological structures of the shoot buds from flowering and non-flowering *P. pygmaeus* were investigated using a stereomicroscope and scanning electron microscope (SEM). The bud samples at three different growth stages were selected to compare transcriptome differences between flowering and non-flowering *P. pygmaeus* by RNA-Seq. The identified unigenes were involved in metabolic synthesis, signal transmission, translation, and other functions based on seven databases. A total of 129 flowering-related genes with 2434 unigenes were screened from transcriptome analysis, which were involved in the photoperiod pathway, vernalization pathway, autonomous pathway, gibberellins (GA) pathway, age pathway, and other pathways. Moreover, the relative expression level of a few key flowering-related genes was verified by *q*RT-PCR, which was in accordance with RNA-Seq.

2. Materials and Methods

2.1. Plant Materials

P. pygmaeus (Miq.) Nakai belongs to Bambusoideae, Gramineae, which has been deposited in International Plant Names Indexe with ID 416341-1 (https://www.ipni.org/n/416341-1). The plant species originated from Nanjing Gulin nursery and was introduced to a bamboo garden of Nanjing Forestry University in Jiangsu Province, China (32°4′44″ N, 118°48′17″ E) in the 1980s [15]. The *P. pygmaeus* plants were grown under the natural environment with an annual average temperature of 15.7 °C and an annual average precipitation of 971.7 mm. They began to flower in 2015 for the first time. The dormant shoot buds (FE), germinated shoots (FM), and flower buds (FL) from 50 one-year-old flowering *P. pygmaeus* plants and the dormant shoot buds (NE), germinated shoots (NM), and leaf buds (NL) from 50 non-flowering plants were harvested in 2016 for morphological and transcriptome comparisons.

2.2. Morphological and Anatomical Characterization

The samples were fixed in 70% FAA solution (70% alcohol:glacial acetic acid:formaldehyde = 90:5:5). The bracts of the samples were stripped under an anatomical microscope (S6D, Leica, Shanghai, China). Then the samples were sliced to 8 μm with a Leica RM 2255 microtome (Leica biosystems Nussloch GmbH, Wetzlar, Germany) by the conventional paraffin sectioning method [16]. The slices were stained using Safranine and Fast Green double dyeing and then photographed under a Leica DM 2500

microscope (Leica Microsystems CMS GmbH, Wetzlar, Germany) [16]. In addition, the samples were dehydrated by ethanol, dried at critical point and sprayed with gold by an ion sputtering instrument. They were then photographed under SEM.

2.3. Sample and Library Preparation

The shoot buds at different developmental stages were rapidly frozen in liquid nitrogen and stored at −80 °C. The plant samples with the five respective biological repeats were sent with dry ice to Novogene (https://en.novogene.com/) for RNA-Seq.

A total amount of 1.5 μg RNA per sample was used as input material for sample preparations. cDNA libraries were generated using NEBNext® Ultra™ RNA Library Prep Kit for Illumina (NEB, New England Biolabs, Ipswich, USA): (1) mRNA was enriched from total RNA with poly-T oligo-attached magnetic beads and was then broken into short segments using divalent cations under elevated temperature. (2) First-strand cDNA was synthesized with random hexamers and M-MuLV reverse transcriptase using enriched mRNA as a template. (3) Second-strand cDNA was synthesized with buffer solution (dNTPs), DNA polymerase I, and RNase H using first-strand cDNA as a template and was then purified by AMPure XP beads to select cDNA fragments of preferentially 150~200 bp in length. (4) The purified double-strand cDNA was repaired by adding A tails at the ends. (5) PCR was performed with Phusion high-fidelity DNA polymerase, universal PCR primers and index primer, and PCR products were purified to obtain the final library by AMPure XP beads. (6) Qubit 2.0 was used for preliminary quantification, and the library was diluted to 1.5 ng/μL. (7) Agilent 2100 was used to assess the quality of the library, and q-PCR was used to accurately quantify the effective concentration of the library (>2 nM). Finally, the prepared library was pair end sequenced with 150 bp by 6× depth using an Illumina Hiseq 2000 platform.

2.4. Quality Control and Transcriptome Assembly

The raw sequencing data was deposited in NCBI SRA with the accession number PRJNA648794. The raw sequencing reads were cleaned by removing adapter sequences, reads with ambiguous N bases, and low quality reads (i.e., the number of bases with quality value Qphred ≤ 20 accounts for more than 50% of the entire reads) with RSeQC [17]. A de novo assembly was performed using Trinity 2.2 with min_kmer_cov set to 2 and all other parameters by default [18]. Different contigs from the same transcript were linked based on double-terminal information, and the transcripts were obtained by further sequence splicing. Then the different transcript sequences of each gene were profiled in a transcript cluster unit by Corset [19]. Finally, the library including irredundant unigenes was constructed.

2.5. Gene Annotation and Differential Gene Expression

All unigenes were aligned to seven major databases using Blast2GO with default parameters [20], including NR (NCBI non-redundant protein sequences), NT (NCBI non-redundant nucleotide sequences), Pfam (Protein family), KOG (Eukaryotic ortholog group), SWISS-PROT (A manually annotated and reviewed protein sequence database), KEGG (Kyoto encyclopedia of genes and genomes), and GO (Gene Ontology). The biology functions of the unigenes were annotated based on functional information of the above databases. The e-value distribution map was calculated and drawn according to NR library comparison annotation, and the screening criteria was set as *e*-value $< 1.0 \times e^{-5}$. The functional annotation of flowering-related unigenes of *P. pygmaeus* was referred from the flowering-related genes identified from *Arabidopsis thaliana*, *Oryza sativa*, *Sorghum bicolor*, and *Brachypodium distachyon*.

The gene expression level in each sample was quantified by RSEM (RNA-Seq by Expectation Maximization) with Bowtie alignment program by default [21]. Differential expression analysis in the comparisons was performed using the DESeq R package based on negative binomial distribution, and *p*-values were adjusted using Benjamini and Hochberg's approach [22]. The unigenes with an adjusted *p*-value < 0.05 were assigned as differentially expressed unigenes (DEUs). GO enrichment analysis of the DEUs was implemented by GOseq based on Wallenius non-central hyper-geometric distribution [23]. KOBAS was used to test the statistical enrichment of the DEUs in KEGG pathways [24]. The unigenes involved in different flowering pathways were clustered based on FPKM (Fragments per Kilobase Million) by Heatmapper (http://www.heatmapper.ca/expression/) with default parameters.

2.6. qRT-PCR Verification

The obtained samples were rapidly frozen in liquid nitrogen and stored at −80 °C for qRT-PCR. The mRNA was extracted by a Column Plant RNAout Kit (CAT#:71203, Tiandz, Beijing, China). The quantity of RNA was determined by Nanodrop 2000c, and the quality of RNA was detected by Agilent 2100. The cDNA was obtained using PrimeScript™ RT reagent Kit with gDNA Eraser (RR047A, Takara, Dalian, China).

The key flowering-related genes, such as *CO*, *FLC*, *FT*, and *SOC1*, which play important roles in several flowering pathways, were chosen for *q*RT-PCR verification. *Tubulin* was used as the internal reference gene [25] and all primers (Supplementary Table S1) were designed using Primer 5.0. An IQ Multicolor real-time PCR automatic amplification apparatus was used for *q*RT-PCR with three biological repeats for each sample. The relative expression level of each gene was calculated using $2^{-\Delta CT}$ [26]. ANOVA ($p < 0.05$) was used to identify significant differences of gene expression among different samples.

3. Results

3.1. Morphological and Anatomical Characterization of the Samples

According to the biological characteristics of bamboo plants, the shoot buds during three different developmental stages, including the FE, FM, and FL from flowering *P. pygmaeus,* and the NE, NM, and NL from non-flowering *P. pygmaeus* were harvested for morphological observation (Figure 1). Morphological phenotypes of the dormant shoot buds were similar in flowering and non-flowering plants: the main axis was short and the upper layer was covered with 7–8 layers of shoot sheath (Figure 2A,E), and the appearance of the apical growth cone was conical (Figure 3A,D). Accompanied with the elongation of the main axis, the germinated shoot buds from most flowering plants began to differentiate, and floret primordia continuously sprouted on both sides of the main axis (Figures 2C and 3B). The morphological characteristics of the germinated shoot buds from a few flowering plants (Figure 2B) were similar with those from non-flowering plants (Figure 2F): with the elongation of principal axis, the tunica cells underwent anticlinal division, the apical growth cones elongated longitudinally (Figure 3E), and bract primordia continuously formed around the growth cones. The flower buds and leaf buds displayed obvious differences in anatomy. The 1–2 cm flower buds developed into a mixed inflorescence with 1–3 spikelets and 9–20 florets (Figure 2D). The appearance of the apical meristem was hemispherical (Figure 3C). However, leaf primordia continuously formed on both sides of the main axis (Figure 2G), and the appearance of the apical meristem was conical in 1–2 cm leaf buds (Figure 3F).

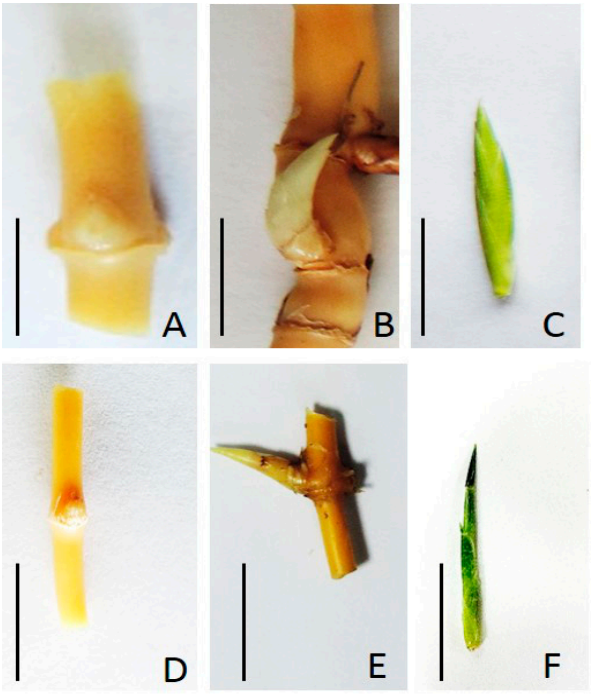

Figure 1. The shoot buds at different development stages. (**A**) Dormant shoot bud of a flowering plant; (**B**) Germinated shoot of a flowering plant; (**C**) Flower bud of a flowering plant; (**D**) Dormant shoot bud of vegetative plant; (**E**) Germinated shoot of a vegetative plant; (**F**) Leaf bud of a vegetative plant. Bar = 1 cm.

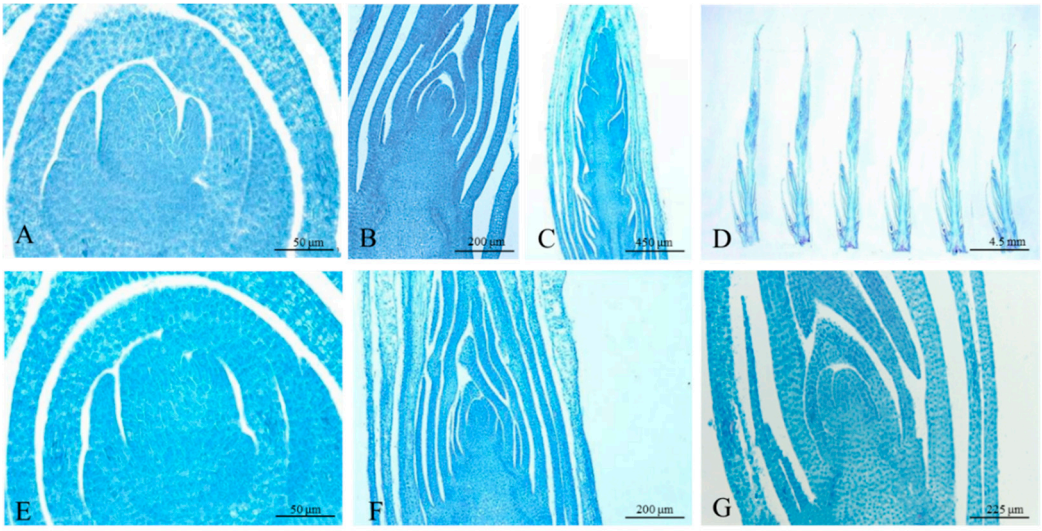

Figure 2. Anatomy of the shoot buds at different development stages. (**A**) Dormant shoot bud of a flowering plant; (**B**,**C**) Germinated shoot of a flowering plant; (**D**) Flower bud of a flowering plant; (**E**) Dormant shoot bud of a vegetative plant; (**F**) Germinated shoot of a vegetative plant; (**G**) Leaf bud of a vegetative plant.

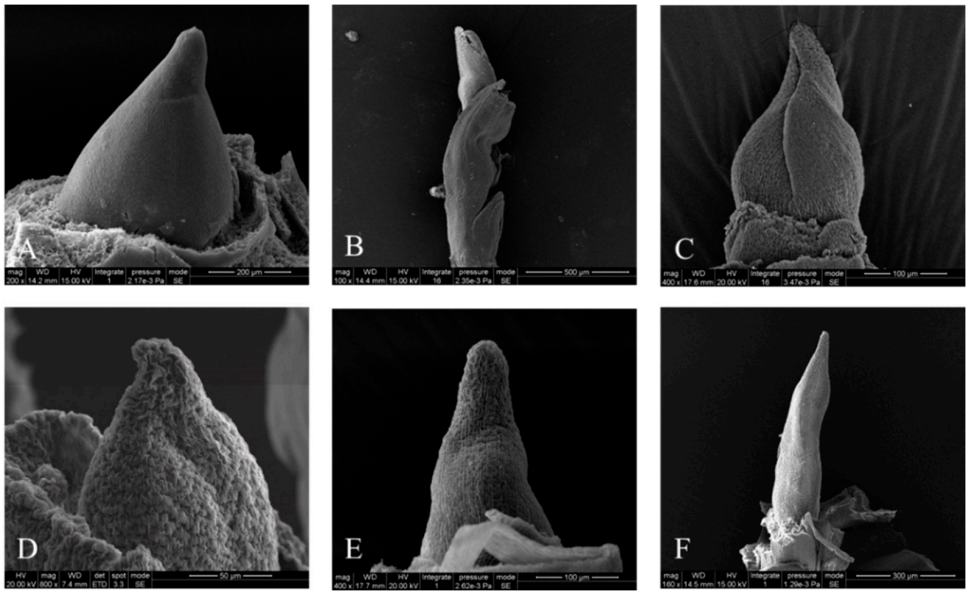

Figure 3. SEM of the shoot buds at different development stages. (**A**) Dormant shoot bud of a flowering plant; (**B**) Germinated shoot of a flowering plant; (**C**) Flower bud of a flowering plant; (**D**) Dormant shoot bud of a vegetative plant; (**E**) Germinated shoot of a vegetative plant; (**F**) Leaf bud of a vegetative plant.

3.2. Data Filtering and Assembly

Transcriptome sequencing information of FE, FM, FL, NE, NM, and NL is shown in Supplementary Table S2. After filtration, the guanine-cytosine (GC) content of clean reads was more than 50%, and the average value of Q30 was more than 90%, which indicated that the clean data can be used for subsequent assembly. A total of 616,137 transcripts were obtained from all samples. Among them, there were 371,978, 109,062, 79,705, 55,392 transcripts with a length of 200–500 bp, 500–1000 bp, 1000–2000 bp, and >2000 bp, respectively (Figure 4A). A total of 364,840 unigenes were obtained by further redundant processing of the transcripts. The 500–2000 bp unigenes accounted for 50.88% of the total unigenes. Specifically, there were 124,007 unigenes with a length of 200–500 bp, 105,748 with 500–1000 bp, 79,693 with 1000–2000 bp, and 55,392 with >2000 bp, respectively (Figure 4B).

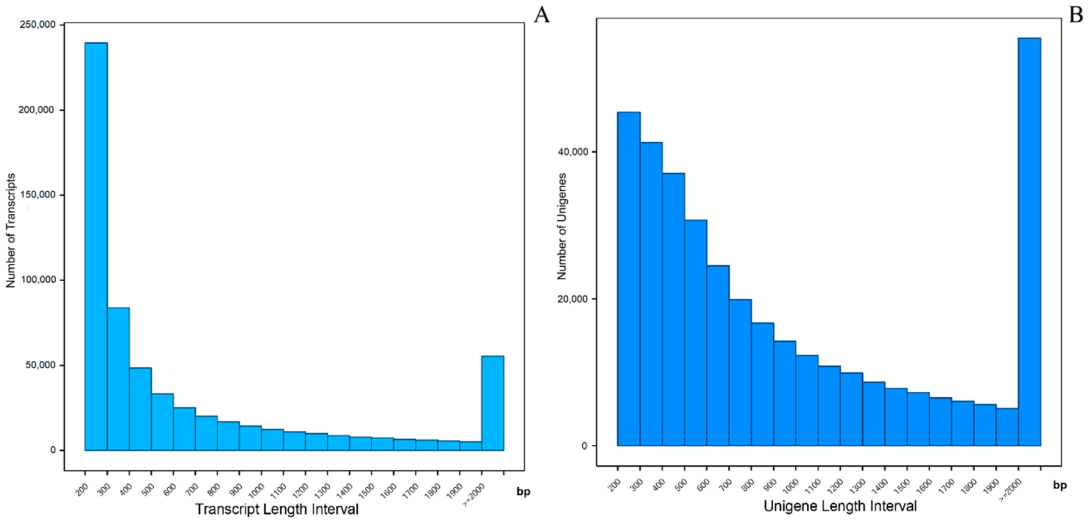

Figure 4. Length distribution of *Pleioblastus pygmaeus* transcripts and unigenes in base pairs (bp). (**A**) Length distribution of *Pleioblastus pygmaeus* transcripts; (**B**) Length distribution of *Pleioblastus pygmaeus* unigenes.

3.3. Gene Annotation

A total of 364,840 irredundant unigenes were obtained based on functional annotations of the seven major databases, including NR, NT, Pfam, KOG, SWISS-PROT, KEGG, and GO. Among them, most unigenes were annotated in the NR database with 201,547 accounting for 55.24% of the total unigenes. It was followed by NT and GO databases with 199,699 and 154,573 unigenes, accounting for 54.73% and 42.36% of the total unigenes, respectively. There were 147,740, 144,866, 76,768, and 54,875 unigenes annotated in Pfam, SWISS-PROT, KEGG, and KOG databases, respectively, which accounted for 40.49%, 39.70%, 21.04%, and 15.04% of the total unigenes, respectively. As many as 30,935 unigenes were shared in the seven databases, accounting for 8.47% of the total unigenes (Supplementary Table S3).

Based on the distribution of e-values in the database, 44.70% of matched sequences showed strong homology (*e*-value < 1.0×10^{-60}), and 55.30% of matched sequences showed general homology (between 1.0×10^{-5} and 1.0×10^{-60}) (Figure 5A). Transcript comparisons indicated that *P. pygmaeus* had the most homologous sequences with *Oryza sativa* (22.70%), followed by *Brachypodium distachyon* (14.73%), *Setaria italica* (11.29%), *Oryza brachyantha* (11.14%), and *Phyllostachys edulis* (3.05%) (Figure 5B). The GO, KOG, and KEGG functional annotations showed that the unigenes were mostly related to cellular process, material metabolism, and genetic information processes. GO analysis indicated that the unigenes with metabolic and synthetic functions were more abundant in flowering plants than in non-flowering plants, which might be related to continuous metabolism in flower bud differentiation. Based on KEGG enrichment analysis, the genes involved in plant hormone signal transduction and circadian rhythm may play an important role in the flowering process of *P. pygmaeus*.

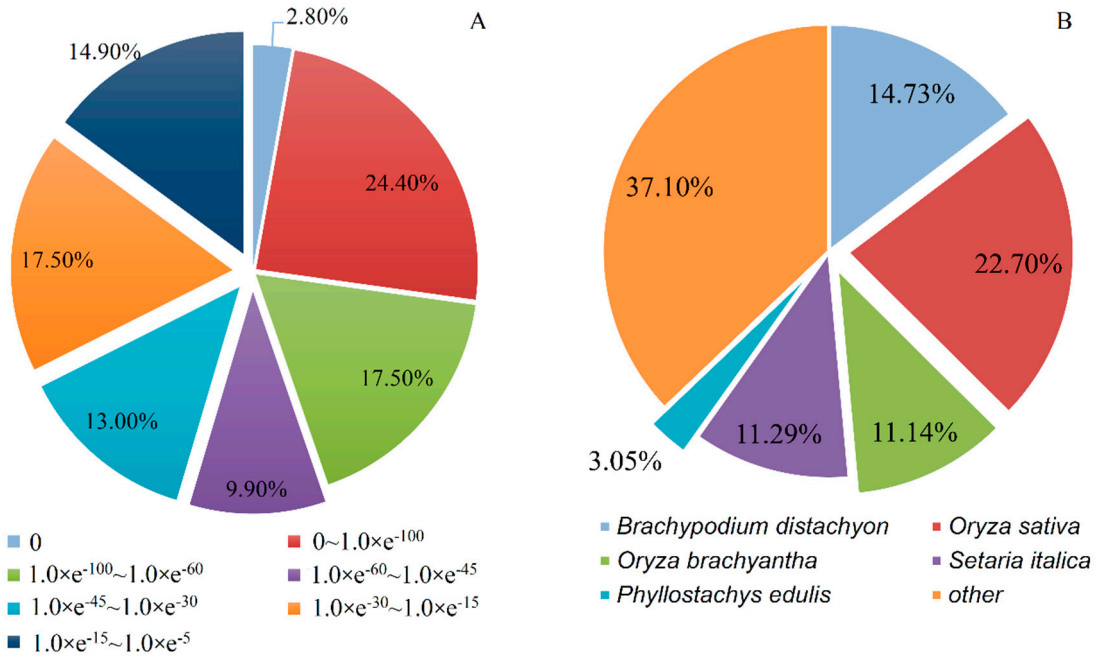

Figure 5. E-value and species distribution of *Pleioblastus pygmaeus* unigenes in NR. (**A**) E-value distribution of *Pleioblastus pygmaeus* unigenes in NR; (**B**) Species distribution of *Pleioblastus pygmaeus* unigenes in NR.

3.4. Differential Gene Enrichment Analysis

To identify differentially expressed flowering-related genes, the transcriptomes of the shoot buds at the same developmental stage from flowering and non-flowering plants were compared (Figure 6). The DEUs in FE vs. NE were mainly involved in metabolic processes and binding agents (Figure 6A). The unigenes were enriched in biological processes and binding in FM vs. NM (Figure 6B), while the unigenes associated with biosynthesis, metabolic processes and catalytic activity were abundant in

FL vs. NL (Figure 6C). These unigenes may be related to metabolism processes during flower bud differentiation and/or flower organ primordium establishment. Moreover, the DEUs in FE vs. FM and NE vs. NM were most abundant in catalytic and binding activity according to GO enrichment analysis (Figure 6D,E). The results indicated that mRNA abundance of the unigenes related to catalytic and binding activity was much higher in flowering *P. pygmaeus* than that in non-flowering plants.

Based on significant enrichment analysis using KEGG, the unigenes in genetic information processing (2675) showed the highest enrichment in FE vs. NE (Supplementary Table S4), which was mainly concentrated in the spliceosome (539), protein processing in the endoplasmic reticulum (502), RNA transport (436), and the secondary enrichment was in metabolism (1650). The highest number of unigenes was also found in genetic information processing (1645) in FM vs. NM (Supplementary Table S5), which mainly included protein processing in the endoplasmic reticulum (412), spliceosome (382), mRNA surveillance pathway (269), and the secondary enrichment was also metabolism (1281). In FL vs. NL (Supplementary Table S6), most enrichment branches were involved in metabolism (2047), which was mainly composed of oxidative phosphorylation (301), pyruvate metadata (242), and glyoxylate and dicarboxylate metabolism (206). A total of 128 DEUs were obtained in the three comparisons, which were mainly involved in cellular processes, environmental information processing, genetic information processing, metabolism and organismal systems. In FE vs. FM, DEUs with maximum enrichment were observed in starch and sucrose metabolism (2233) (Supplementary Table S7), including starch and sucrose metabolism (546), phenylpropanoid biosynthesis (427), amino sugar and nucleotide sugar metabolism (405). In NE vs. NM (Supplementary Table S8), DEUs were most enriched in starch (1919), including starch and sucrose metabolism (371), phenylpropanoid biosynthesis (289), and amino sugar and nucleotide sugar metabolism (252), which was similar to FE vs. FM.

Ge et al. (2017) suggested that the floral process of *Phyllostachys pubescens* was related to plant–pathogen interactions, protein processing in the endoplasmic reticulum, and plant hormone signal transaction [27]. In all comparisons (Supplementary Table S9), the plant–pathogen interaction was only enriched in FE vs. FM, which was not significant yet, indicating the blossoming process of *P. pygmaeus* had a low relationship with plant–pathogen interactions. Protein processing in the endoplasmic reticulum was not significantly enriched in FE vs. NE and FM vs. NM, but it was highly enriched in FL vs. NL, which indicated that there was more protein processing in flower buds than in rhizome buds. Significant enrichment of plant hormone signal transduction was present in each group, which indicated that plant hormone signal transduction plays an important role in the flowering process of *P. pygmaeus*.

In addition, the q-values of the plant circadian rhythm pathway in FM vs. NM and FL vs. NL were 0.29 and 0.04, respectively (Supplementary Table S9). The enrichment of the pathway was significantly different in flower buds and leaf buds. The q-values of FE vs. FM and NE vs. NM were 1.00 and 0.11, respectively (Supplementary Table S9), which indicated that the enrichment degree of differentially expressed genes in the circadian rhythm pathway was much greater in flowering *P. pygmaeus* than that in non-flowering plants. The above results indicated that the plant circadian rhythm pathway was critical in the flower formation process of *P. pygmaeus*.

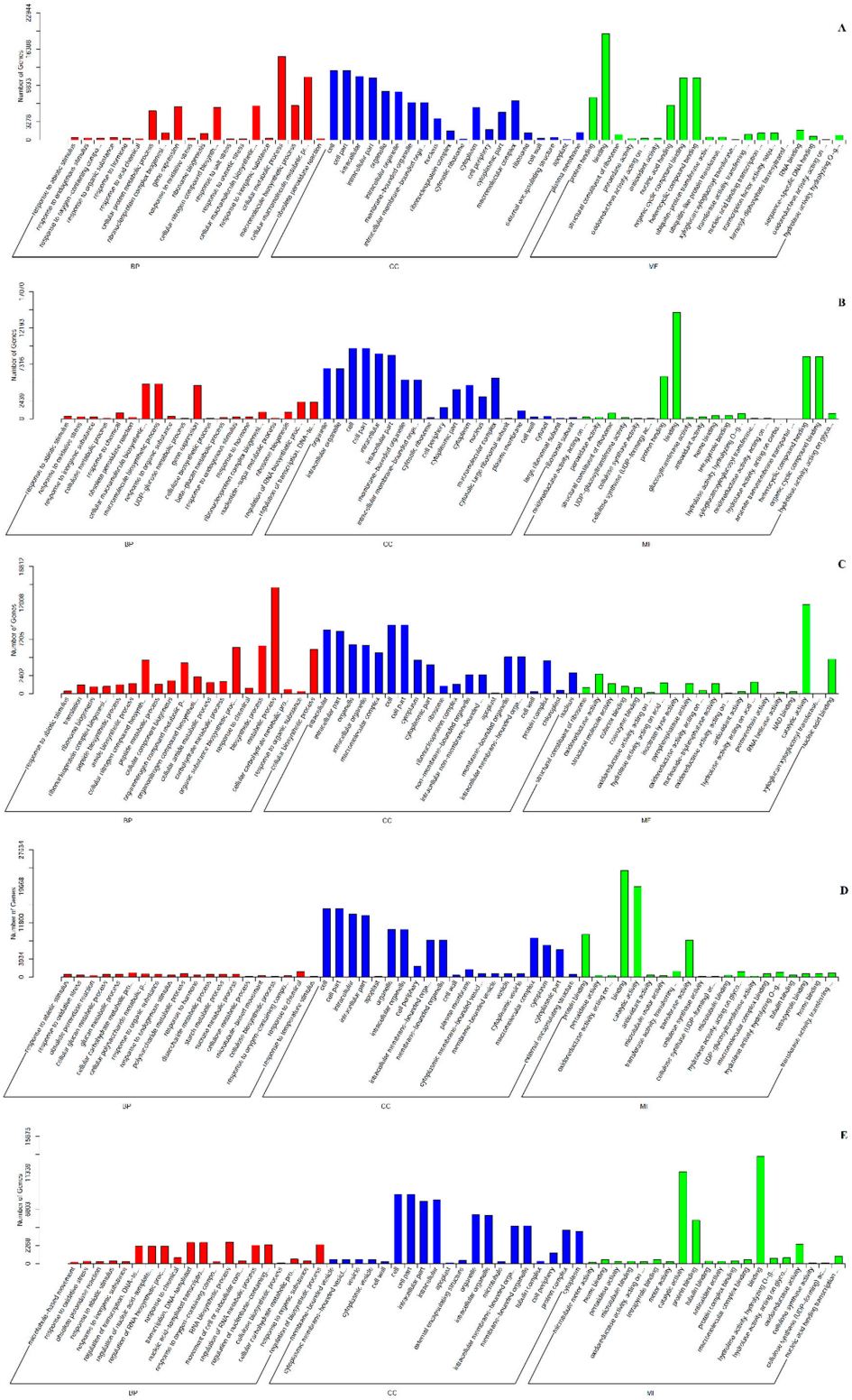

Figure 6. Differential expressed unigenes based on GO function annotation. (**A**) DEUs in FE vs. NE; (**B**) DEUs in FM vs. NM; (**C**) DEUs in FL vs. NL; (**D**) DEUs in FE vs. FM; (**E**) DEUs in NE vs. NM. FE, Dormant shoot buds of flowering plants; FM, Germinated shoots of flowering plants; FL, Flower buds of flowering plants; NE, Dormant shoot buds of vegetative plants; NM, Germinated shoots of vegetative plants; NL, Leaf buds of vegetative plants; BP, Biological Process; CC, Cellular Component; MF, Molecular Function.

3.5. Expression Analysis of Key Genes Involved in Floral Development

The flowering process was co-regulated by multiple regulation pathways in plants. A total of 129 flowering-related genes with 2434 unigenes were identified from transcriptome analysis of *P. pygmaeus*. There were 52 genes with 647 unigenes, 19 genes with 298 unigenes, 6 genes with 93 unigenes, 20 genes with 1023 unigenes, 21 genes with 179 unigenes, 4 genes with 71 unigenes, and 7 genes with 123 unigenes, in the photoperiod pathway, vernalization pathway, autonomous pathway, gibberellins pathway, age pathway, pentose phosphate pathway, and flowering signal integrator, respectively (Supplementary Table S10, Figure 7). The highly expressed unigenes were most abundant in flowering P. pygmaeus. In particular, there were more unigenes involved in the photoperiod pathway expressed in FE and FL, such as *CO*, *PHY*, TCP, etc., compared to those in NE and NL. Moreover, a few *SPLs*, such as *SPL3*, *SPL4*, *SPL5*, etc., and flowering signal integrators, such as *FT*, *FD*, *SOC1*, etc., were highly expressed in flower buds (Figure 7).

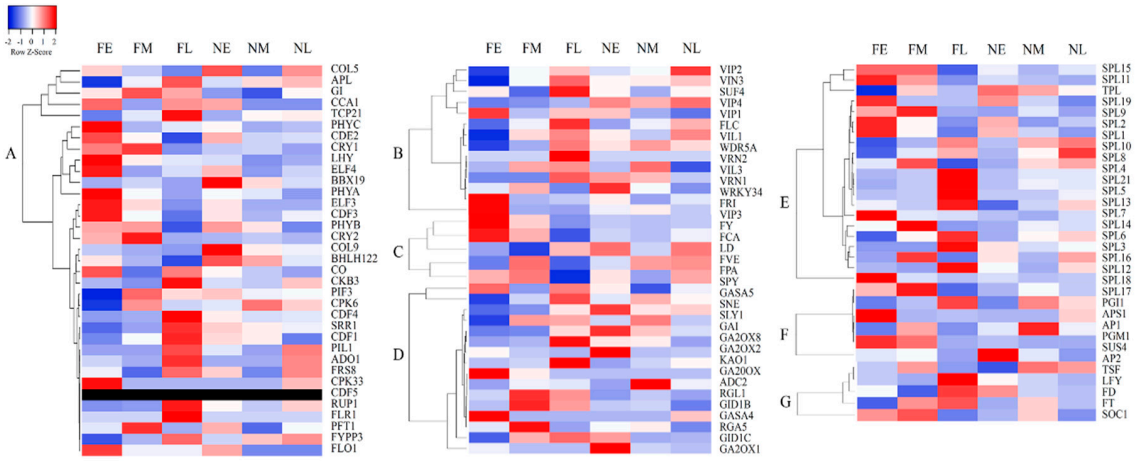

Figure 7. Clustering of gene expression profiles. (**A**) Photoperiod pathway; (**B**) Vernalization pathway; (**C**) Autonomous pathway; (**D**) Gibberellins pathway; (**E**) Age pathway; (**F**) Pentose phosphate pathway; (**G**) Flowering signal integrator. FE, Dormant shoot buds of flowering plants; FM, Germinated shoots of flowering plants; FL, Flower buds of flowering plants; NE, Dormant shoot buds of vegetative plants; NM, Germinated shoots of vegetative plants; NL, Leaf buds of vegetative plants. The raw z-score is determined based on the FPKM values, red and blue colors represent highly and lowly-expressed unigenes, black shows that the FPKM of the unigene was not detected.

3.6. RNA-Seq Expression Validation of Key Genes Involved in Floral Development

As shown in Figure 8, the relative expression level of *CO*, *SOC1*, and *FT* was significantly higher in flowering *P. pygmaeus* than that in non-flowering plants, while the expression of *FLC* was lower in flowering *P. pygmaeus* than that in non-flowering plants. The expression of *CO* was significantly higher in FE, FM, and FL than that in NE, NM, and NL. The expression of *SOC1* was significantly higher in FM and FL than that in NM and NL. *CO* and *SOC1* were limited or rarely expressed in dormant shoots, while they were highly induced in germinated shoots and flower/leaf buds. The expression of *SOC1* increased more significantly than that of *CO*. *CO* and *SOC1* were both expressed in flower buds and gradually decreased with the completion of floral organ formation, indicating that they played an important role in flower transition of *P. pygmaeus*. The expression of the *FT* gene showed an upward trend throughout the whole flowering process and was significantly higher in flower buds, indicating that *FT* played an important role in flower vessel maturation of *P. pygmaeus*. However, the expression of *FLC* was significantly lower in FE, FM, and FL than that in NE, NM, and NL, indicating that *FLC* was inhibited in the flower transition of *P. pygmaeus*.

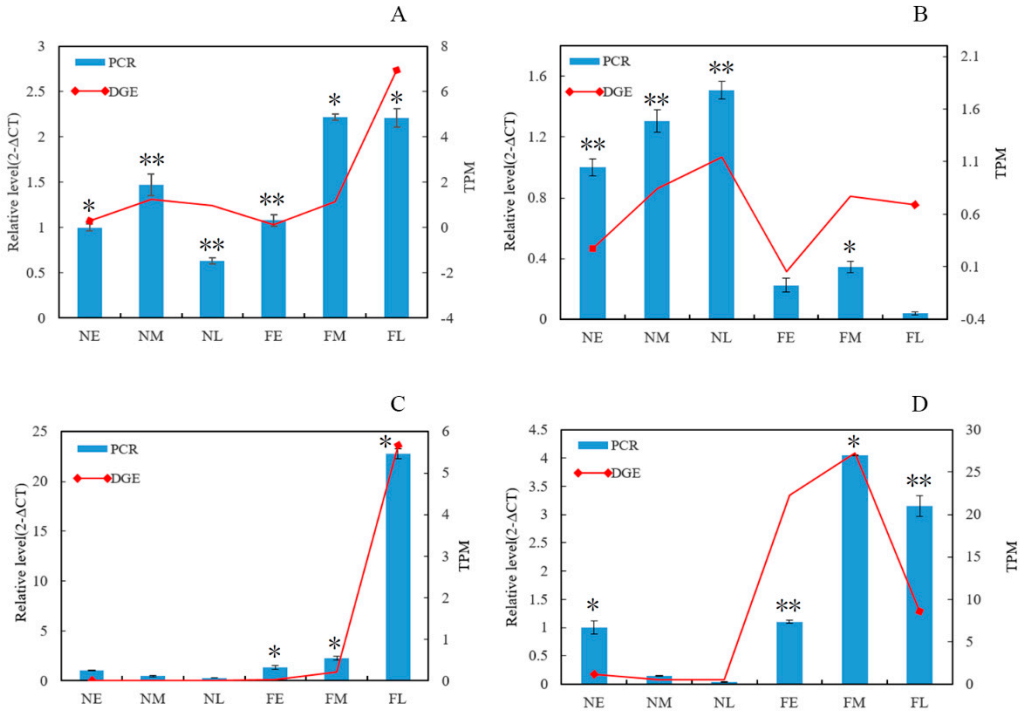

Figure 8. RNA-seq expression validation of *CO*, *FLC*, *FT* and *SOC1* genes. (**A**) Relative expression of *CO* gene; (**B**) Relative expression of *FLC* gene; (**C**) Relative expression of *FT* gene; (**D**) Relative expression *SOC1* gene. Mean values and deviations were calculated from three independent biological experiments. * indicates $p < 0.05$, ** indicates $p < 0.01$. PCR, relative expression level by *q*RT-PCR; DGE, differentially gene expression by RNA-Seq; TPM, Transcripts Perkilobase Million.

4. Discussion

Plants accomplish the transition from vegetative growth to reproductive growth by flowering. The flowering process is a complex process in higher plants, which is regulated by different flowering pathways, including the photoperiod pathway, vernalization pathway, autonomous pathway, GA pathway, age pathway, etc. [28]. In this study, a total of 129 flowering-related genes with 2434 unigenes involved in different flowering pathways were screened from transcriptome comparisons of the shoot buds from flowering and non-flowering *P. pygmaeus*.

The photoperiod pathway is a key genetic mechanism regulating flowering in plants [29]. A total of 52 genes with 647 unigenes involved in the photoperiod pathway were found in the transcriptomes of *P. pygmaeus* in the study, including *CO*, *FT*, *SOC1*, *LFY* and other genes. In the photoperiod pathway, the *FT* gene is a direct target gene of the transcriptional regulator, *CO* [30,31]. Under long sunlight conditions, sustained expression of *CO* can activate the expression of *FT* [32], meanwhile *FT* can activate *SOC1* and *LFY* to promote flowering [33].

The vernalization pathway is regulated by low-temperature signals. A total of 19 genes with 298 unigenes related to vernalization were found in transcription analysis of *P. pygmaeus* in the study, including key flowering-related genes, *FLC*, *VRN1*, *VRN2*, etc. [34]. *FLC* belongs to the MADS-box family, which is responsible for maintaining the nutritional state of bud tips [35]. *FLC* can control flowering by inhibiting the expression of *FT* and *SOC1* [36]. *VRN1* also belongs to the MADS family and is homologous with the *AP1* gene from *Arabidopsis thaliana* (L.) Heynh., 1842, which can be induced by low temperature [37]. *VRN2* is a flowering repressor that is down-regulated by vernalization and can inhibit the expression of *VRN1* [38]. Additionally, 127 unigenes identified from *P. pygmaeus* transcriptomes are highly homologous with *VIN1*, *VIN2*, and *VIN3*, which also inhibit *FLC* expression at low temperature [39].

The autonomous pathway is an independent floral induction pathway. A series of key flowering-related genes, such as *FCA*, *FPA*, *FLD*, *FLK*, *FY*, *FVE*, and *LD*, have been identified in the pathway [40,41]. There were 93 homologous unigenes related to the autonomous pathway found in the transcriptional analysis of *P. pygmaeus* in the study, including *FCA* (12), *FPA* (15), *FLK* (39), *FY* (11), *FVE* (6), and *LD* (10). *FCA* and *FPA* encode RNA binding proteins containing plant-specific RNA recognition motifs (RRMs), which can inhibit the accumulation of *FLC* [42,43]. *LD* is the first independent gene cloned from *A. thaliana* in the pathway [44]. *FLK*, *FY*, and *FVE* encode RNA binding proteins that inhibit expression of *FLC* [42,45].

The GA pathway can affect flowering induction and organ development by regulating endogenous hormones. A total of 20 genes with 1023 unigenes involved in the pathway were found in the transcriptome comparisons of *P. pygmaeus* in the study. GA promotes flowering by increasing expression of the integron genes (e.g., *SOC1*, *LFY* and *FT*) in *A. thaliana* [46]. *GAI* and *RGA* genes from the GRAS family can inhibit the GA response in plants [47]. There were six *GAI* unigenes and five *RGA* (*RGA1/2/3/4/5*) with 892 unigenes, accounting for 87.19% of the total unigenes in the GA pathway of *P. pygmaeus*. It was reported that the *GID* receptor can detect GA activity in *Oryza sativa* [48]. There were two *GID1* receptors found in the transcription analysis of *P. pygmaeus*, including *GID1B* and *GID1C*.

The ageing pathway is an endogenous way to control flowering time through plant growth. In the study, 21 *SPL* genes (*SPL1–SPL19*, and *SPL21*) with 179 unigenes were found in transcriptome comparisons of *P. pygmaeus*. A few *SPLs*, as key TFs in the ageing pathway, can promote the transformation from vegetative growth to reproductive growth of plants [49]. It was reported that several *SPLs* can positively induce the *FT* gene, and its activity increased with age [50]. A few *SPLs* can further activate the expression of flowering-related genes such as *LFY*, *AP1* and *FUL* [51]. In addition, some *SPLs* may be indirectly involved in the photoperiod and GA pathways [52,53].

As a key gene in the photoperiod pathway, *CO* directly regulates the expression of the *FT* gene, which promotes flowering [30,31]. *FLC* is an inhibitory factor in flowering regulation and participates in vernalization and autonomic pathways. *FLC* negatively regulates the expression of *FT* and *SOC1* in *A. thaliana* [36]. The *FT* gene is a conservative activator of flowering and differently affects the flowering of short-day and long-day plants [32,33]. In *A. thaliana*, the FT protein interacts with the FD protein to activate *AP1* expression and initiate the transition from vegetative growth to reproductive growth [54]. The *SOC1* gene is a TF of the MADS-box family. The expression of the *SOC1* gene in the stem tip meristem increases in the flower formation process [33]. Moreover, the *FT* gene and *FLC* gene can affect the expression of *SOC1* in *A. thaliana* [33,36]. To verify RNA-Seq results, the relative expression level of the key flowering-related genes was quantified by qRT-PCR, which was in accordance with RNA-Seq. The expression of *CO*, *SOC1*, and *FT* was significantly higher in flowering *P. pygmaeus* than that in non-flowering plants, while *FLC* expression displayed the opposite phenomenon. The results indicated that they play an important role in regulating the flowering process of *P. pygmaeus*.

5. Conclusions

In the study, morphological characteristics of the shoot buds at different developmental stages from flowering and non-flowering *P. pygmaeus* were revealed. The dormant shoot buds had a similar morphological phenotype in flowering and non-flowering plants, while there were obvious differences in germinated shoot buds and flower/leaf buds. Meanwhile, the transcriptomes of the shoot buds were compared to screen flowering-related genes in *P. pygmaeus*. The identified unigenes mainly function in metabolic synthesis, signal transmission, translation, and others based on gene annotation. A total of 2434 unigenes involved in the flowering process were screened from transcriptome comparisons of the shoot buds from flowering and non-flowering *P. pygmaeus*, including 647, 298, 93, 1023, 179 unigenes in the photoperiod pathway, vernalization pathway, autonomous pathway, GA pathway, and ageing pathway, respectively. In particular, the DEUs associated with circadian rhythm and plant hormone signal transduction play an important role in flower transition of *P. pygmaeus*. Moreover, *q*RT-PCR

results indicated that the relative expression level of a few key flowering-related genes such as *CO*, *SOC1*, and *FT* was significantly higher in flowering *P. pygmaeus* than that in non-flowering plants, which was in accordance with RNA-Seq analysis. This study enriches the reproductive biology of small-size bamboo plants and provides a scientific basis for further understanding of floral transition in bamboo plants.

Supplementary Materials: The following are available online at http://www.mdpi.com/1999-4907/11/11/1229/s1. Supplementary Table S1. The Primer pairs of key flowering-related genes; Supplementary Table S2. Summary of RNA-Seq libraries for five biological replicates of the shoot buds at different growth stages of *Pleioblastus pygmaeus;* Supplementary Table S3. Function annotation of the transcriptomes of the shoot buds at different growth stages of *Pleioblastus pygmaeus* in different databases; Supplementary Tables S4–S8. Differential expressed unigenes based on KEGG function annotation in transcriptome comparisons of FE (Dormant shoot buds of flowering plants) vs. NE (Dormant shoot buds of vegetative plants), FM (Germinated shoots of flowering plants) vs. NM (Germinated shoots of vegetative plants), FL (Flower buds of flowering plants) vs. NL (Leaf buds of vegetative plants), FE (Dormant shoot buds of flowering plants) vs. FM (Germinated shoots of flowering plants), NE (Dormant shoot buds of vegetative plants) vs. NM (Germinated shoots of vegetative plants), respectively; Supplementary Table S9. The significantly enriched pathway-terms in transcriptome comparisons of *Pleioblastus pygmaeus;* Supplementary Table S10. Flowering-related unigenes identified in different flowering pathways of *Pleioblastus pygmaeus*.

Author Contributions: S.L. conceived and designed the research. W.Y. conducted experiments, analyzed data and wrote the manuscript. C.L., L.R., Y.W. and L.Z. conducted experiments and analyzed data. Y.D. revised the manuscript. All authors have read and agreed to the published version of the manuscript.

Funding: This work was financially supported by National Natural Science Foundation of China (31870595; 32001292), Natural Science Foundation of Jiangsu Province (BK20190748) and Priority Academic Program Development of Jiangsu Higher Education Institutions (PAPD).

Conflicts of Interest: The authors declare no conflict of interest.

Abbreviations

DEUs	differentially expressed unigenes
TF	Transcription factor
SEM	Scanning electron microscope
GA	Gibberellins
FE	Dormant shoot buds of flowering plants
FM	Germinated shoots of flowering plants
FL	Flower buds of flowering plants
NE	Dormant shoot buds of vegetative plants
NM	Germinated shoots of vegetative plants
NL	Leaf buds of vegetative plants
NR	NCBI non-redundant protein sequences
NT	NCBI non-redundant nucleotide sequences
Pfam	Protein family
KOG	Eukaryotic ortholog group
KEGG	Kyoto encyclopedia of genes and genomes
GO	Gene ontology
GC	guanine-cytosine
bp	base pair
RSEM	RNA-Seq by Expectation Maximization
FPKM	Fragments per Kilobase Million
TPM	Transcripts Perkilobase Million
RRMs	RNA recognition motifs

References

1. Liese, W.; Köhl, M. *Bamboo: The Plant and Its Uses*; Springer: Heidelberg/Berlin, Germany, 2015.
2. Zheng, X.; Lin, S.Y.; Fu, H.J.; Wang, Y.W.; Ding, Y.L. The bamboo flowering cycle sheds light on flowering diversity. *Front. Plant Sci.* **2020**, *11*, 381. [PubMed]

3. Jiao, Y.L.; Hu, Q.T.; Zhu, Y.; Zhu, L.F.; Ma, T.F.; Zeng, H.Y.; Zang, Q.L.; Li, L.; Lin, X.C. Comparative transcriptomic analysis of the flower induction and development of the Lei bamboo (*Phyllostachys violascens*). *BMC Bioinfor.* **2019**, *20*, 687.
4. Rout, G.R.; Das, P. Somatic embryogenesis and in vitro flowering of 3 species of bamboo. *Plant Cell Rep.* **1994**, *13*, 683–686. [PubMed]
5. Fan, T.T.; Guo, Z.H.; Fu, H.J.; Zhang, L.; Ding, Y.L. Germination and storage characteristics of *Pleioblastus pygmaeus* pollen. *Forest Res.* **2018**, *31*, 180–185.
6. Lin, S.Y.; Li, J.; Zhao, R.; Dong, X.B.; Ding, Y.L. The development of flowering bud differentiation and male gametophyte of *Bambusa multiplex*. *J. Nanjing For. Univ. Nat. Sci.* **2015**, *39*, 51–56.
7. Waikhom, S.D.; Louis, B.; Roy, P.; Singh, W.M.; Bharwaj, P.K.; Talukdar, N.C. Scanning electron microscopy of pollen structure throws light on resolving Bambusa–Dendrocalamus complex: Bamboo flowering evidence. *Plant Syst. Evol.* **2014**, *300*, 1261–1268.
8. Saitoh, T.; Seiwa, K.; Nishiwaki, A. Importance of physiological integration of dwarf bamboo to persistence in forest understorey: A field experiment. *J. Ecol.* **2002**, *90*, 78–85.
9. Prasun, B.; Sukanya, C.; Smritikana, D.; Amita, P.; Malay, D. Bamboo flowering from the perspective of comparative genomics and transcriptomics. *Front. Plant Sci.* **2016**, *7*, 1900.
10. Zhao, H.S.; Gao, Z.M.; Wang, L.; Wang, J.L.; Wang, S.B.; Fei, B.H.; Chen, C.H.; Shi, C.C.; Liu, X.C.; Zhang, H.L.; et al. Chromosome-level reference genome and alternative splicing atlas of moso bamboo (*Phyllostachys edulis*). *Gigascience* **2018**, *7*, giy115.
11. Li, Y.; Zhang, C.X.; Yang, K.B.; Shi, J.J.; Gao, Z.M. De novo sequencing of the transcriptome reveals regulators of the floral transition in *Fargesia macclureana* (Poaceae). *BMC Genom.* **2019**, *20*, 1035.
12. Gao, J.; Zhang, Y.; Zhang, C.L.; Qi, F.Y.; Li, X.P.; Mu, S.H.; Peng, Z.H.; Gaquerel, E. Characterization of the floral transcriptome of Moso bamboo (*Phyllostachys edulis*) at different flowering developmental stages by transcriptome sequencing and RNA-Seq analysis. *PLoS ONE* **2014**, *9*, e98910.
13. Zhang, X.M.; Zhao, L.; Larson-Rabin, Z.; Li, D.Z.; Guo, Z.H.; Nitabach, M.N. De novo sequencing and characterization of the floral transcriptome of *Dendrocalamus latiflorus* (Poaceae: Bambusoideae). *PLoS ONE* **2012**, *7*, e42082.
14. Peng, Z.H.; Lu, Y.; Li, L.B.; Zhao, Q.; Jiang, Z.H. The draft genome of the fast-growing non-timber forest species moso bamboo (*Phyllostachys heterocycla*). *Nat. Genet.* **2013**, *45*, 456–461. [PubMed]
15. Lin, S.Y.; Fan, T.T.; Jiang, M.Y.; Zhang, L.; Zheng, X.; Ding, Y.L. The revision of scientific names for three dwarf bamboo species (cultivar) based on the floral morphology. *J. Nanjing For. Univ. Nat. Sci.* **2017**, *41*, 189–193.
16. Su, J.L.; Lin, S.Y.; Shi, W.S.; Wang, X.; Zheng, X.; Wan, Y.W.; Ding, Y.L. Anatomical observation and three-dimensional construction of leaf blades from six bamboos. *J. Nanjing For. Univ. Nat. Sci.* **2020**, *44*, 47–53.
17. Wang, L.G.; Wang, S.Q.; Li, W. RSeQC: Quality control of RNA-seq experiments. *Bioinformatics* **2012**, *28*, 2184–2185.
18. Grabherr, M.G.; Haas, B.J.; Yassour, M.; Levin, J.Z.; Thompson, D.A.; Amit, I.; Adiconis, X.; Fan, L.; Raychowdhury, R.; Zeng, Q.D. Full-length transcriptome assembly from RNA-Seq data without a reference genome. *Nat. Biotechnol.* **2011**, *29*, 644–652.
19. Davidson, N.M.; Oshlack, A. Corset: Enabling differential gene expression analysis for de novo assembled transcriptomes. *Genome Biol.* **2014**, *15*, 410.
20. Götz, S.; García-Gómez, J.M.; Terol, J.; Williams, T.D.; Nagaraj, S.H.; Nueda, M.J.; Robles, M.; Talón, M.; Dopazo, J.; Conesa, A. High-throughput functional annotation and data mining with the Blast2GO suite. *Nucleic Acids Res.* **2008**, *36*, 3420–3435.
21. Li, B.; Dewey, C.N. RSEM: Accurate transcript quantification from RNA-Seq data with or without a reference genome. *BMC Bioinform.* **2011**, *12*, 323.
22. Wang, L.K.; Feng, Z.X.; Wang, X.; Wang, X.W.; Zhang, X.G. DEGseq: An R package for identifying differentially expressed genes from RNA-seq data. *Bioinformatics* **2010**, *26*, 136–138. [PubMed]
23. Young, M.D.; Wakefield, M.J.; Smyth, G.K.; Oshlack, A. Gene ontology analysis for RNA-seq: Accounting for selection bias. *Genome Biol.* **2010**, *11*, R14. [PubMed]
24. Mao, X.Z.; Cai, T.; Olyarchuk, J.G.; Wei, L.P. Automated genome annotation and pathway identification using the KEGG Orthology (KO) as a controlled vocabulary. *Bioinformatics* **2005**, *21*, 3787–3793. [PubMed]

25. Fan, C.J.; Ma, J.M.; Guo, Q.R.; Li, X.T.; Wang, H.; Lu, M.Z. Selection of Reference Genes for Quantitative Real-Time PCR in Bamboo (*Phyllostachys edulis*). *PLoS ONE* **2013**, *8*, e56573.
26. Livak, K.J.; Schmittgen, T.D. Analysis of relative gene expression data using real-time quantitative PCR and the 2(−delta delta c(t)) method. *Methods* **2001**, *25*, 402–408.
27. Ge, W.; Zhang, Y.; Cheng, Z.C.; Hou, D.; Gao, J. Main regulatory pathways, key genes and microRNAs involved in flower formation and development of Moso bamboo (*Phyllostachys edulis*). *Plant Biotechnol. J.* **2017**, *15*, 82–96.
28. Putterill, J.; Laurie, R.; Macknight, R. It's time to flower: The genetic control of flowering time. *Bioessays* **2004**, *26*, 363–373.
29. Coupland, G. Regulation of flowering by photoperiod in *Arabidopsis*. *Plant Cell Environ.* **2010**, *20*, 785–789.
30. Valverde, F.; Mouradov, A.; Soppe, W.; Ravenscroft, D.; Samach, A.; Coupland, G. Photoreceptor regulation of CONSTANS protein in photoperiodic flowering. *Science* **2004**, *303*, 1003–1006.
31. An, H.; Roussot, C.; Suárez-López, P.; Corbesier, L.; Vincent, C.; Piñeiro, M.; Hepworth, S.; Mouradov, A.; Justin, S.; Turnbull, C.; et al. CONSTANS acts in the phloem to regulate a systemic signal that induces photoperiodic flowering of *Arabidopsis*. *Development* **2004**, *131*, 3615–3626.
32. Castillejo, C.; Pelaz, S. The balance between *CONSTANS* and *TEMPRANILLO* activities determines *FT* expression to trigger flowering. *Curr. Biol.* **2008**, *18*, 1338–1343. [PubMed]
33. Lee, J.E.; Lee, I. Regulation and function of *SOC1*, a flowering pathway integrator. *J. Exp. Bot.* **2010**, *61*, 2247–2254. [PubMed]
34. Sheldon, C.C.; Finnegan, E.J.; Dennis, E.S.; Peacock, W.J. Quantitative effects of vernalization on *FLC* and *SOC1* expression. *Plant J.* **2010**, *45*, 871–883.
35. Dennis, E.S.; Peacock, W.J. Epigenetic regulation of flowering. *Curr. Opin. Plant Biol.* **2007**, *10*, 520–527. [PubMed]
36. Bastow, R.; Mylne, J.S.; Lister, C.; Lippman, Z.; Martienssen, R.A.; Dean, C. Vernalization requires epigenetic silencing of *FLC* by histone methylation. *Nature* **2004**, *427*, 164–167.
37. Aaron, G.; James, P.W.; Dennis, E.S.; Ben, T. The molecular biology of seasonal flowering-responses in *Arabidopsis* and the cereals. *Ann. Bot.* **2009**, *103*, 1165–1172.
38. Yan, L.L.; Loukoianov, A.; Blechl, A.; Tranquilli, C.; Ramakrishna, W.; SanMiguel, P.; Bennetzen, J.L.; Echenique, V.; Dubcovsky, J. The wheat *VRN2* gene is a flowering repressor down-regulated by vernalization. *Science* **2004**, *303*, 1640–1644.
39. Finnegan, E.J.; Kovac, K.A.; Jaligot, E.; Sheldon, C.C.; Peacock, W.J.; Dennis, E.S. The downregulation of FLOWERING LOCUS C (*FLC*) expression in plants with low levels of DNA methylation and by vernalization occurs by distinct mechanisms. *Plant J.* **2010**, *44*, 420–432.
40. Winichayakul, S.; Beswick, N.L.; Dean, C.; Macknight, R.C. Components of the *Arabidopsis* autonomous floral promotion pathway, *FCA* and *FY*, are conserved in monocots. *Funct. Plant Biol.* **2005**, *32*, 345–355.
41. Jang, Y.H.; Park, H.Y.; Kim, S.K.; Hwan, L.J.; Chung, S.M.; Soo, C.Y.; Kyung-Hee, P.; Jeong-Kook, K. Survey of rice proteins interacting with *OsFCA* and *OsFY* proteins which are homologous to the *Arabidopsis* flowering time proteins, *FCA* and *FY*. *Plant Cell Physiol.* **2009**, *50*, 1479–1492.
42. Lim, M.H.; Kim, J.; Kim, Y.S.; Chung, K.S.; Seo, Y.H.; Lee, I.; Kim, J.; Hong, C.B.; Kim, H.J.; Park, C.M. A new Arabidopsis gene, *FLK*, encodes an RNA binding protein with K homology motifs and regulates flowering time via FLOWERING LOCUS C. *Plant Cell* **2004**, *16*, 731–740. [PubMed]
43. Simpson, G.G.; Quesada, V.; Henderson, I.R.; Dijkwel, P.P.; Dean, C. RNA processing and *Arabidopsis* flowering time control. *Biochem. Soc. Trans.* **2004**, *32*, 565–566. [PubMed]
44. Lee, I.; Aukerman, M.J.; Gore, S.L.; Lohman, K.N.; Michaels, S.D.; Weaver, L.M.; John, M.C.; Feldmann, K.A.; Amasino, R.M. Isolation of LUMINIDEPENDENS: A gene involved in the control of flowering time in *Arabidopsis*. *Plant Cell* **1994**, *6*, 75–83. [PubMed]
45. Marquardt, S.; Boss, P.K.; Hadfield, J.; Dean, C. Additional targets of the *Arabidopsis* autonomous pathway members, *FCA* and *FY*. *J. Exp. Bot.* **2006**, *57*, 3379–3386. [PubMed]
46. Gocal, G.F.; Sheldon, C.C.; Gubler, F.; Moritz, T.; Bagnall, D.J.; MacMillan, C.P.; Li, S.F.; Parish, R.W.; Dennis, E.S.; Weigel, D.; et al. GAMYB-like genes, flowering, and gibberellin signaling in *Arabidopsis*. *Plant Physiol.* **2001**, *127*, 1682–1693. [PubMed]
47. Peng, J.; Carol, P.; Richards, D.E.; King, K.E.; Cowling, R.J.; Murphy, G.P.; Harberd, N.P. The *Arabidopsis GAI* gene defines a signaling pathway that negatively regulates gibberellin responses. *Genes Dev.* **1997**, *11*, 3194–3205. [PubMed]

48. Ueguchi-Tanaka, M.; Ashikari, M.; Nakajima, M.; Itoh, H.; Katoh, E.; Kobayashi, M.; Chow, T.Y.; Hsing, Y.C.; Kitano, H.; Yamaguchi, I. GIBBERELLIN INSENSITIVE DWARF1 encodes a soluble receptor for gibberellin. *Nature* **2005**, *437*, 693–698.
49. Fornara, F.; Coupland, G. Plant phase transitions make a SPLash. *Cell* **2009**, *138*, 625–627.
50. Khan, M.R.G.; Ai, X.Y.; Zhang, J.Z. Genetic regulation of flowering time in annual and perennial plants. *Wiley Interdiscip. Rev. RNA* **2014**, *5*, 347–359.
51. Yamaguchi, A.; Wu, M.F.; Yang, L.; Wu, G.; Poethig, R.S.; Wagner, D. The microRNA-regulated SBP-Box transcription factor *SPL3* is a direct upstream activator of *LEAFY*, *FRUITFULL*, and *APETALA1*. *Dev. Cell* **2009**, *17*, 268–278.
52. Unte, U.S.; Sorensen, A.M.; Pesaresi, P.; Gandikota, M.; Leister, D.; Saedler, H.; Huijser, P. *SPL8*, an SBP-box gene that affects pollen sac development in *Arabidopsis*. *Plant Cell* **2003**, *15*, 1009–1019. [PubMed]
53. Riese, M.; Zobell, O.; Saedler, H.; Huijser, P. SBP-domain transcription factors as possible effectors of cryptochrome-mediated blue light signalling in the moss *Physcomitrella patens*. *Planta* **2008**, *227*, 505–515. [PubMed]
54. Komeda, Y. Genetic regulation of time to flower in *Arabidopsis thaliana*. *Annu. Rev. Plant Biol.* **2004**, *55*, 521–535. [PubMed]